Analysis of 2D Singular Effect on Nonlinear Wave Forces with Application of Scaled Boundary FEM

Bin Teng* and Yixin Qian

State Key Laboratory of Coastal and Offshore Engineering, Dalian University of Technology, Dalian 116023, China

Highlights:

- Nonlinear diffraction problem of a 2D box are solved with application of the Scaled Boundary FEM
- Radial functions are obtained analytically for velocity potential and its derivatives of on body boundary
- Analytic method is used to integrate the singular derivative of velocity potential at corners and to improve the accuracy of nonlinear forces.

1 Introduction

Nonlinear effect has been acknowledged as an assignable component in hydrodynamic analysis. To obtain the quantities of high order force, derivatives of velocity potential have the priority to be accurately worked out.

However, difficulty exists in the calculation of tangential velocity on body surface, especially in constant panel method (CPM). This problem is relieved with the development of high order boundary element method (HOBEM). Compared with CPM, HOBEM improves the accuracy and convergence for general cases (Choi et al[1]), but still remains aporias. One of them is the singular effect of corners, which has been ignored or simplified technically in traditional approaches.

Attributed to the discontinuity of boundary condition, singularity usually occurs at sharp corners of bodies. Since the velocities soar to infinite in the vicinity of corners, this kind of singular behavior could no longer be precisely described by discrete method merely. In HOBEM, the variation trend of derivatives on body surface is interpolated with linear or quadratic curve, which disobeys the theoretical analysis as well. These errors contribute to the divergence of nonlinear forces as pointed out by Zhao and Faltinsen[2], and Teng et al[3].

Thus, analytic approach is supposed to provide more convincing explanation on singularity. Scaled Boundary FEM (SBFEM) is such a numerical approach that provides analytic means to study on this project. In SBFEM, scaled coordinates are founded, and the solution is analytic in the radial direction, named as 'radial function'. The radial function has an explicit formulation with fine smoothness that has effect in computing the singularity. In addition, the integration of derivatives of velocity potential at corners can be computed analytically with the radial function. Results show Scaled Boundary FEM has higher efficiency and accuracy compared with HOBEM for body with corners.

2 Scaled Boundary FEM solution of potential flow problem

2.1 Scaled coordinates

SBFEM defines the domain by scaling similar-curve relative to a scaling center (x_0, z_0). Take a 2-D domain with a breach for example (Fig.1). The scaling center is set at the corner, where is supposed to exist a singular problem. The circumferential coordinate S is anticlockwise along the similar-curve, and the radial coordinate ξ is the ratio of similar-curve to the circumferential boundary (Fig. 1-b).

The Cartesian coordinates are transformed to the scaled coordinates with the following formulas

$$\begin{cases} x_s(\xi,s) = x_0 + \xi \cdot \left[N(s)\right] \cdot \{x - x_0\} \\ z_s(\xi,s) = z_0 + \xi \cdot \left[N(s)\right] \cdot \{z - z_0\} \end{cases} \tag{1}$$

where $[N(s)]$ is the shape function, (x, z) are the Cartesian coordinates of the discrete nodes. What is worth mentioning is, unlike boundary element method, only the circumferential boundary is discretized in this approach (Fig. 1-b).

2.2 Scaled-Boundary FEM equation

An approximate solution of ϕ is described as a product of circumferential function $S(s)$ and radial function $a(\xi)$

$$\phi(\xi,s) = S(s) \cdot a(\xi) = \left[N(s)\right] \cdot \{a(\xi)\} \tag{2}$$

in which analytic solutions are adapted for the radial function $\{a(\xi)\}$, and numerical discretization with shape function $[N(s)]$ is applied for the circumferential function.

By applying the weighted residual method, an integral equation is achieved for the fluid domain Ω surrounded by the body boundary Γ_b $\left(\xi_I \le \xi \le \xi_E, s = s_0 \text{ or } s_1\right)$ and a single piecewise-smooth curve S $\left(\xi=\xi_I \text{ or } \xi_E, s_0 \le s \le s_1\right)$

$$\iint_{\Omega} \nabla w(\xi,s) \cdot \nabla \phi(\xi,s) \cdot \left|J(s)\right| d\xi ds = \oint_{S+\Gamma_b} w(\xi,s) \cdot v_n(\xi,s) d\Gamma \tag{3}$$

where the weight function shares the form of velocity potential $w(\xi, s) = [N(s)]\ \{w(\xi)\}$, ξ_I and ξ_E are the radial coordinates of the inner and outer boundaries of the computation domain, which are selected as zero and unit in this paper, and s_0 and s_1 are the circumferential coordinates of two ends of curve S.

As a result of separation of variables, the integral of S is calculated into constant coefficient matrix $[E_0]$, $[E_1]$ and $[E_2]$ beforehand.

Finally a Scaled Boundary FEM equation could be obtained due to the arbitrariness of $\{w(\xi)\}$,

$$[E_0]\xi^2 \{a(\xi)\}_{\xi\xi} + \left([E_0] + [E_1]^T - [E_1]\right)\xi \{a(\xi)\}_{\xi} - [E_2]\{a(\xi)\} = \xi \{f_s(\xi)\} \tag{4}$$

along with the circumferential boundary condition

$$[E_0]\xi_I \{a(\xi_I)\}_{\xi} + [E_1]^T \{a(\xi_I)\} = \int_{s_0}^{s_1} \left[N(s)\right]^T v_n(\xi_I, s) \tau^{\xi} ds$$

$$[E_0]\xi_E \{a(\xi_E)\}_{\xi} + [E_1]^T \{a(\xi_E)\} = \int_{s_0}^{s} \left[N(s)\right]^T v_n(\xi_E, s) \tau^{\xi} ds$$

The radial boundary condition is contained in the nonhomogeneous term in Eq. (4), representing the motion of body surface. Detailed formula derivations are available in previous articles [4].

2.3 The radial function and singularity of velocity

The Scaled Boundary equation (4) is solved analytically with eigenvalue method

$$\{a(\xi)\} = [A]\xi^{[\Lambda]}\{c\} + \{a(\xi)\}^S \tag{5}$$

where the diagonal matrix $[\Lambda]$ is made up of the nonnegative eigenvalues λ_1, λ_2, λ_3, … of Eq. (4). The coefficient matrix [A] has been worked out along with the eigenvalues, while the vector $\{c\}$ remains to be determined. Particular solution $\{a(\xi)\}^S$ is to satisfy the nonhomogeneous term.

Then, the radial function at *node i* is formulated in a power series

$$a(\xi)_i = \sum_{j=1}^{m} A_{i,j} c_j \cdot \xi^{\lambda_j} + a(\xi)_i^S \tag{6}$$

It can be found that λ_1 is between 0 and 1 when (x_0, z_0) is at a corner.

The tangential derivative of velocity potential on body surface can be calculated analytically by

$$v_\tau(\xi)=\frac{\partial\phi}{\partial\tau}=\frac{\left[N(s)\right]}{\sqrt{(x-x_0)^2+(z-z_0)^2}}\cdot\{a(\xi)\}_\xi+\frac{\left[N(s)\right]_s}{\sqrt{(x-x_0)_s^2+(z-z_0)_s^2}}\frac{1}{\xi}\cdot\{a(\xi)\},\quad (s=s_0\ or\ s_1) \tag{7}$$

which will include singularities at a corner. The second derivatives have a similar form containing $\{a(\xi)\}_{\xi\xi}$ in addition.

3 Numerical Results and Discussion

A comparison study on the second order exciting force on a 2D box is made between the Scaled Boundary FEM and a HOBEM model with Rankine source. Velocity potential derivatives and wave forces on a 2-D floating box are calculated. The box is in a water depth of d, and has a draft of T/d=0.2 and half width of B/d=0.2. The whole computational domain is divided into 5 subdomains, and the radiation boundaries are set at x=+/-1.2d. To simulate the singularity property, the scaled centers of the two subdomains adjoin to the body are set at the submerged corners (Fig. 2). Three meshes with 46, 93 and 140 elements are applied for SBFEM, and four meshes with 216, 448, 680 and 920 elements are applied for the HOBEM model for convergent studies.

For convenience of analysis, the second order exciting force is divided into three components:

$$f^{(2)}=f_{22}+f_{21,a}+f_{21,b}=2\mathrm{i}\rho\omega\int_{S_M}\phi^{(2)}\mathrm{n}ds-\frac{\rho\nu}{4}(\phi^{(1)}\phi^{(1)}\mathrm{n}|_{x=X_L}+\phi^{(1)}\phi^{(1)}\mathrm{n}|_{x=X_R})-\frac{\rho}{4}\int_{S_M}\nabla\phi^{(1)}\cdot\nabla\phi^{(1)}\mathrm{n}ds \tag{8}$$

where f_{22} is the term from the second order potential, $f_{21,\mathrm{a}}$ the term from waterline integration and $f_{21,\mathrm{b}}$ the term from the integration of first derivative of velocity over body surface, Figs. 3 and 4 are validations of the former two parts, and show that the agreements are very good even with the coarse meshes.

Since the singularity of velocity causes noticeable divergence, $f_{21,\mathrm{b}}$ deserves a convergence research. In the SBFEM model, an analytic method is used for the integration of the square of tangential derivative of velocity potential on body surface

$$f_{21,b}=-\frac{\rho}{4}\int_{S_M}\left[\left(\overline{v}_n+v_n^S\right)^2+\left(\overline{v}_\tau+v_\tau^S\right)^2\right]\cdot\vec{\mathrm{n}}ds=-\frac{\rho}{4}\int_0^1\left[\left(v_n^S(\xi)\right)^2+\left(\overline{v}_\tau(\xi)+v_\tau^S(\xi)\right)^2\right]\cdot\vec{\mathrm{n}}\tau^S d\xi \tag{9}$$

where v_n and v_τ and are the normal and tangential derivatives of velocity potential on body surface. The former is known and the latter is expressed by Eq. (7). The overline and superscript S represent the components of velocity potential satisfying the homogeneous and nonhomogeneous body boundary conditions in Eq. (4) accordingly.

Figs. 5 and 6 are convergent studies on HOBEM and SBFEM, and show that the SBFEM converges more quickly. Fig. 7 shows the comparison between SBFEM and HOBEM with the finest meshes. It can be seen that the result of SBFEM is noticeably larger than that of HOBEM. We suppose that the difference is due to the methods in treatment of the $\xi^{-1/3}$ singularity of fluid velocity at the corner.

Fig. 8 is the comparison of the second order mean drift forces by SBFEM with mesh 3 and HOBEM with mesh 4. Similar conclusion can be seen.

4 Conclusions

On basis of SBFEM, research on the singular problems of corners is carried out. We proposed the analytic expressions for first and second derivatives of velocity potential on body surface, which is superior to the discrete expressions by HOBEM. Hence, the pressure integration on body surface are implemented analytically, with the singular feature adequately considered. Numerical examinations demonstrate the results of SBFEM converge more quickly than those of HOBEM for a body with sharp corner.

References

1. Choi Y R, Hong S Y, Choi H S. An analysis of second-order wave forces on floating bodies by using a higher-order boundary element method, Ocean Engineering, 2000, 28: 117-138.
2. Zhao R and Faltinsen O M, Interaction between Current, Wave and Marine Structures, Proc. 5th Int. Conf. on Numerical Ship Hydrodynamics, 1989, 513-525, Hiroshima.
3. Teng B, Bai W, Dong G H, Simulation of Second-order Radiation of 3D Bodies in Time Domain by a B-spline Method, Proc. of ISOPE，2002, 3, 487-493, Kyushu.
4. Deeks A J, Cheng L, Potential flow around obstacles using the scaled boundary finite-element method, International Journal for Numerical Methods in Fluids, 2003, 41(7), 721-741.

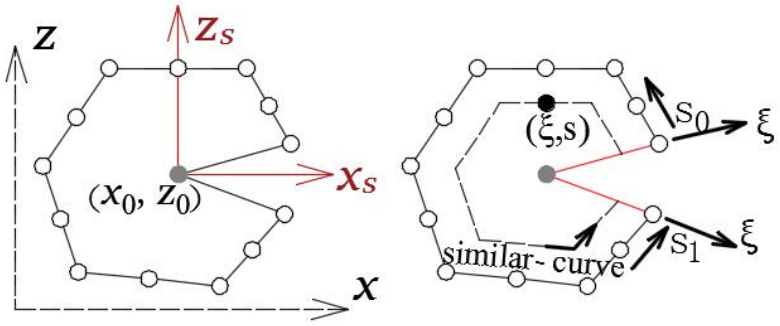

(a) Cartesian coordinate system (b) Scaled coordinate system

Fig.1 Discretization and coordinate transformation

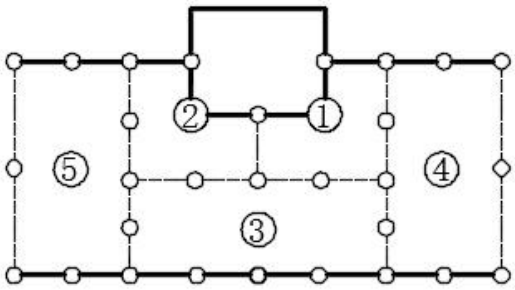

Fig.2 The discretization for SBFEM

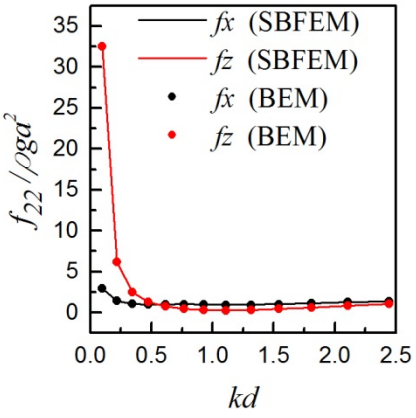

Fig.3 The term of 2nd-order potential

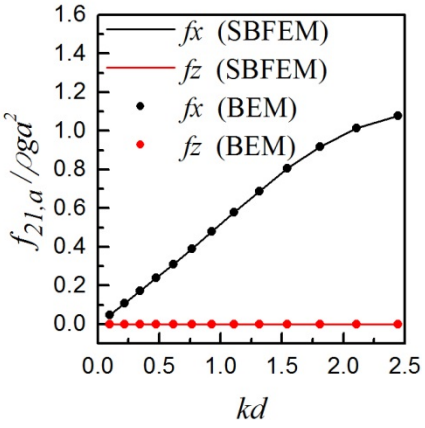

Fig.4 The term on waterline

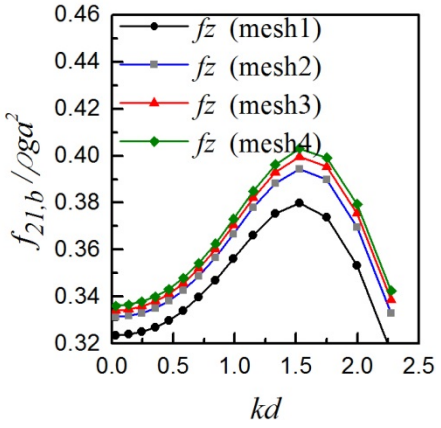

Fig. 5 Convergence of $f_{21,b}$ (HOBEM)

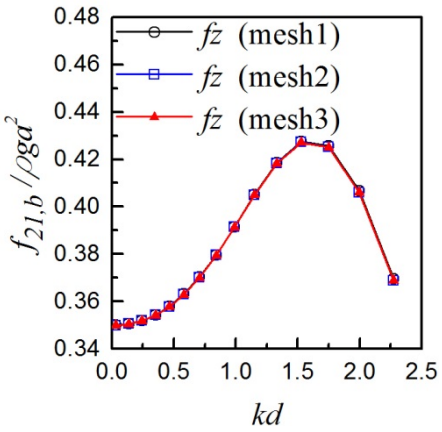

Fig. 6 Convergence of $f_{21,b}$ (SBFEM)

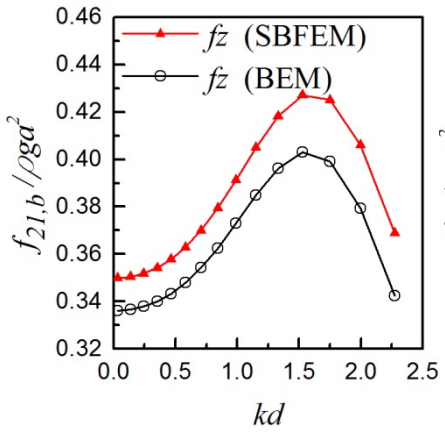

Fig. 7 Comparison of $f_{21,b}$

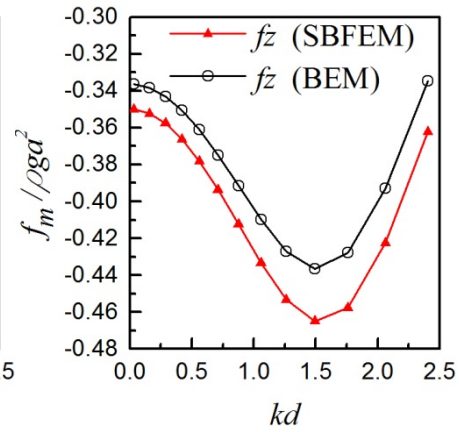

Fig. 8 2nd-order mean force